AFRL-RB-WP-TP-2011-3021

SYSTEM DESIGN AND MODELING OF A THERMALLY ACTIVATED RECONFIGURABLE WING (Postprint)

Gregory W. Reich and James Joo

Advanced Structural Concepts Branch
Structures Division

Richard Beblo and Darrel Robertson

University of Dayton Research Institute

JANUARY 2011
Interim Report

AIR FORCE RESEARCH LABORATORY
AIR VEHICLES DIRECTORATE
WRIGHT-PATTERSON AIR FORCE BASE, OH 45433-7542
AIR FORCE MATERIEL COMMAND
UNITED STATES AIR FORCE

REPORT DOCUMENTATION PAGE

Form Approved
OMB No. 0704-0188

1. REPORT DATE *(DD-MM-YY)*	2. REPORT TYPE	3. DATES COVERED *(From - To)*
January 2011	Conference Paper Postprint	01 September 2009 – 31 August 2010

4. TITLE AND SUBTITLE
SYSTEM DESIGN AND MODELING OF A THERMALLY ACTIVATED RECONFIGURABLE WING (Postprint)

5a. CONTRACT NUMBER
In-House

5b. GRANT NUMBER

5c. PROGRAM ELEMENT NUMBER
0602202F

6. AUTHOR(S)
Gregory W. Reich and James Joo (Structures Division, Advanced Structural Concepts Branch (AFRL/RBSA))
Richard Beblo and Darrel Robertson (University of Dayton Research Institute)

5d. PROJECT NUMBER
A03Q

5e. TASK NUMBER
N/A

5f. WORK UNIT NUMBER
A03Q0G

7. PERFORMING ORGANIZATION NAME(S) AND ADDRESS(ES)

Advanced Structural Concepts Branch (AFRL/RBSA)
Structures Division
Air Vehicles Directorate, Air Force Research Laboratory
Wright-Patterson Air Force Base, OH 45433-7542
Air Force Materiel Command, United States Air Force

University of Dayton Research Institute
300 College Park Avenue
Dayton, OH 45469

8. PERFORMING ORGANIZATION REPORT NUMBER

9. SPONSORING/MONITORING AGENCY NAME(S) AND ADDRESS(ES)

Air Force Research Laboratory
Air Vehicles Directorate
Wright-Patterson Air Force Base, OH 45433-7542
Air Force Materiel Command
United States Air Force

10. SPONSORING/MONITORING AGENCY ACRONYM(S)
AFRL/RBSA

11. SPONSORING/MONITORING AGENCY REPORT NUMBER(S)
AFRL-RB-WP-TP-2011-3021

12. DISTRIBUTION/AVAILABILITY STATEMENT
Approved for public release; distribution unlimited.

13. SUPPLEMENTARY NOTES
PAO Case Number: 88ABW 2010-2993, cleared 04 June 2010. ©2010 ASME. The U.S. Government is joint author of the work and has the right to use, modify, reproduce, release, perform, display, or disclose the work. Published in the Proceedings of the ASME 2010 Conference on Smart Materials, Adaptive Structures and Intelligent Systems, Sept. 28-Oct. 1, 2010, Philadelphia, PA. Document contains color.

14. ABSTRACT
Reconfigurable structures such as morphing aircraft generally require an on board energy source to function. Frictional heating during the high speed deployment of a blunt nosed low speed reconnaissance air vehicle can provide a large amount of thermal energy during a short period of time. This thermal energy can be collected, transferred, and utilized to reconfigure the deployable aircraft. Direct utilization of thermal energy has the ability to significantly decrease or eliminate the losses associated with converting thermal energy to other forms, such as electric. The following work attempts to describe possible system designs and components that can be utilized to transfer the thermal energy harvested at the nose of the aircraft during deployment to internal components for direct thermal actuation of a reconfigurable wing structure. A model of a loop heat pipe is presented and used to predict the time-dependant transfer of energy. Previously reported thermal profiles of the nose of the aircraft, calculated based on trajectory and mechanical analysis of the actuation mechanism, are reviewed and combined with the model of the thermal transport system providing a system level feasibility investigation and design tool. The efficiency, implementation, benefits, and limitations of the direct use thermal system are discussed and compared with currently utilized systems.

15. SUBJECT TERMS

16. SECURITY CLASSIFICATION OF:			17. LIMITATION OF ABSTRACT:	18. NUMBER OF PAGES	19a. NAME OF RESPONSIBLE PERSON (Monitor)
a. REPORT	b. ABSTRACT	c. THIS PAGE			Dr. James Joo
Unclassified	Unclassified	Unclassified	SAR	14	19b. TELEPHONE NUMBER *(Include Area Code)* N/A

Standard Form 298 (Rev. 8-98)
Prescribed by ANSI Std. Z39-18

Proceedings of the ASME 2010 Conference on Smart Materials, Adaptive Structures and Intelligent Systems
SMASIS2010
September 28 – October 1, 2010, Philadelphia, Pennsylvania, USA
SMASIS2010-3636

SYSTEM DESIGN AND MODELING OF A THERMALLY ACTIVATED RECONFIGURABLE WING

Richard Beblo, Darrel Robertson
University of Dayton Research Institute
Dayton, OH, USA 45469

James Joo, Brian Smyers, Gregory Reich
Air Force Research Laboratory
Wright-Patterson AFB, OH, USA 45433

ABSTRACT

Reconfigurable structures such as morphing aircraft generally require an on board energy source to function. Frictional heating during the high speed deployment of a blunt nosed low speed reconnaissance air vehicle can provide a large amount of thermal energy during a short period of time. This thermal energy can be collected, transferred, and utilized to reconfigure the deployable aircraft. Direct utilization of thermal energy has the ability to significantly decrease or eliminate the losses associated with converting thermal energy to other forms, such as electric. The following work attempts to describe possible system designs and components that can be utilized to transfer the thermal energy harvested at the nose of the aircraft during deployment to internal components for direct thermal actuation of a reconfigurable wing structure. A model of a loop heat pipe is presented and used to predict the time dependant transfer of energy. Previously reported thermal profiles of the nose of the aircraft calculated based on trajectory and mechanical analysis of the actuation mechanism are reviewed and combined with the model of the thermal transport system providing a system level feasibility investigation and design tool. The efficiency, implementation, benefits, and limitations of the direct use thermal system are discussed and compared with currently utilized systems.

NOMENCLATURE

A area over which Q is prescribed
C Sutherland's constant, 120 for air
C_f coefficient of friction in supersonic flow
D diameter of the vehicle
H enthalpy
M Mach number of vehicle
P pressure
Pr Prandtl's number
Q heat energy
Re Reynold's number
St Stanton's number
T temperature
U_v maximum vapor velocity in the heat pipe
f location of Uv
h effective heat transfer coefficient
hfg latent heat of vaporization of the working fluid
k thermal conductivity
q heat flux
u velocity
v velocity
x, y, z spatial coordinates

α thermal diffusivity
γ ratio of specific heats, C_p/C_v
ε porosity of the heat pipe wick
θ angle between the stagnation and the evaluated points
μ dynamic viscosity
ρ density
ϕ normalized length of the evaporator

subscripts

0	reference quantity
1	free stream quantity
2	flow behind the shock wave
∞	free stream quantity
c	condenser section of heat pipe
e	evaporator section of heat pipe
in	quantity entering the heat pipe
inj	injection quantity
out	quantity exiting the heat pipe
ref	reference quantity
stag	stagnation point quantity
surface	heat pipe outer surface
v	vapor
w	heat pipe wick

wa	heat pipe wall
wl	liquid material in heat pipe wick
ws	solid material in heat pipe wick
wwc	wall/wick interface in the condenser
wwe	wall/wick interface in the evaporator

INTRODUCTION

Morphing and reconfigurable aircraft in recent years have been the topic of much research due to their adaptability both from efficiency and capability perspectives. One such mission that would greatly benefit from reconfigurability is the high speed delivery of low speed intelligence, surveillance, and reconnaissance (ISR) air vehicles. The ideal ISR asset is one that does not require constant maintenance to maintain system readiness, such as keeping onboard batteries constantly charged while the vehicle is in storage, and has as small as possible delay between storage and deployment, such as waiting for batteries to charge once the need for the vehicle arises. Weighing these two objectives, taking advantage of the benefits of reconfigurability while maintaining system readiness, energy harvesting quickly seems like an optimum solution.

Current ISR vehicles, namely those falling into the broad class of unmanned aerial vehicles (UAVs), are optimized for low speed/high endurance flight. As a result, these aircraft require long flight times to reach destinations that are significant distances from their take off points. Large ISR UAVs are deployed at high altitude servicing a large general area under standing orders with smaller ISR UAVs deployed by ground troops supporting more direct mission objectives. While the smaller UAVs deployed in the field serve to support missions with little advanced notice, they also suffer from limited capabilities due to size and weight restrictions associated with ground transportation. Large UAVs have significantly greater capabilities, however they are not very portable and thus must fly from either their current location or a central base to the desired target, adding time before the asset is in the desired position.

To overcome these two challenges, a medium sized ISR UAV transported to the desired location and deployed by a high speed aircraft has been proposed. Such a vehicle would maintain the functionality afforded by size while having a low "time on target" time. Such a design, however, requires that the vehicle be packaged in a way as to allow transportation by another vehicle and then deploy upon release from the transport vehicle. The most notable challenges associated with this are the folding of the aircraft wings. Deployment of folded wings, in turn, require purposely designed mechanical linkages and actuators and an energy source to drive them. To supply the energy required, direct energy harvesting is proposed.

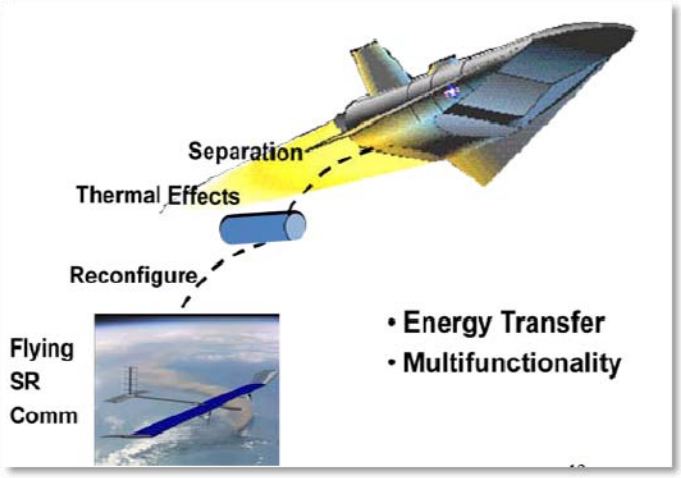

Figure 1: Proposed deployable ISR asset scheme [12]

Above Mach 1.0, a significant amount of thermal energy is produced at the nose of the vehicle due to compression of the atmosphere. Since conversion of thermal energy to other forms, such as electric through the use of thermoelectric or pyroelectric materials, necessarily involves high losses due to conversion efficiencies of the materials, it is desirable to investigate a way to utilize the thermal energy directly, directing the thermal energy to desired locations within the vehicle rather than converting it to other forms. Presented are the results of ongoing efforts in the feasibility and design of such a system.

SYSTEM DESIGN

A conceptual reconfigurable system proposed in this paper is shown in Figure 2. It is composed of thermal transport system and mechanical actuation system. Thermal energy from the environment is directly transferred without energy conversion to trigger the reconfiguration. Each system is represented using an energy metric to optimize the performance of the entire system, the thermal energy modeling of the heat pipe is described in the following section.

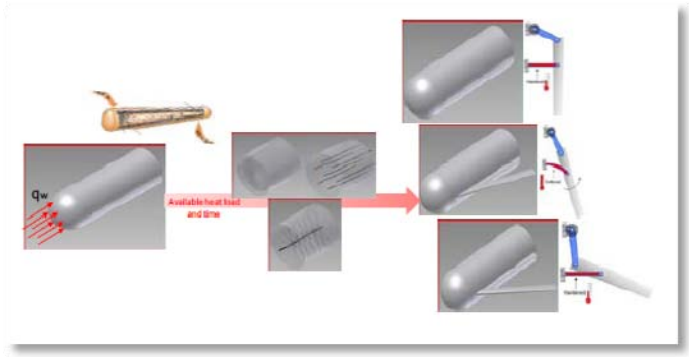

Figure 2: Thermally activated reconfigurable system

Thermal Transport System

The most efficient method of transporting thermal energy over relatively long distances is through the use of a heat pipe or thermal siphon. Heat pipes work by using energy input at one end, the evaporator section, to convert a working fluid to vapor. The vapor is then forced to the opposite end of the heat pipe by pressure differences and condenses, releasing thermal energy in the process. The condensed fluid then returns to the evaporator section through gravity. Alternatively, loop or solid state heat pipes have a wick structure on the inside of the heat pipe , typically a porous sintered metal material, that allows condensed fluid to flow back to the evaporator through capillary action, allowing the heat pipe to function against gravity, such as referenced in Figure 3. Heat pipes can also be arranged side by side with a single covering forming flat plate heat pipes that can be contoured to match the shape of the nose of the vehicle and can be designed to operate in almost any temperature regime, making them an ideal choice for the proposed concept.

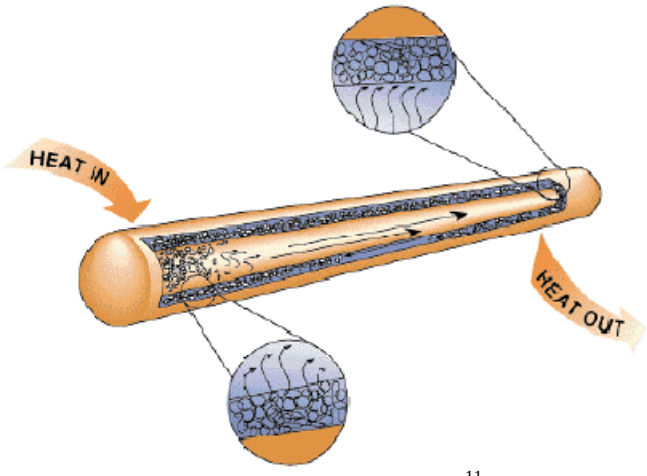

Figure 3: Heat pipe construction[11]

Mechanical Actuation System

A simple non-monolithic compliant mechanism in Figure 4 was proposed as a reconfiguration system because of its multi-functionality (structure and mechanism) and simplicity (passive actuation without active control). Directly transferred heat energy is stored inside a compliant member and is used to trigger the deployment at a specific time. Other concepts such as a system using shape memory wire have been explored but are not mentioned in this paper because our focus is in the concept development of the system not in a component design.

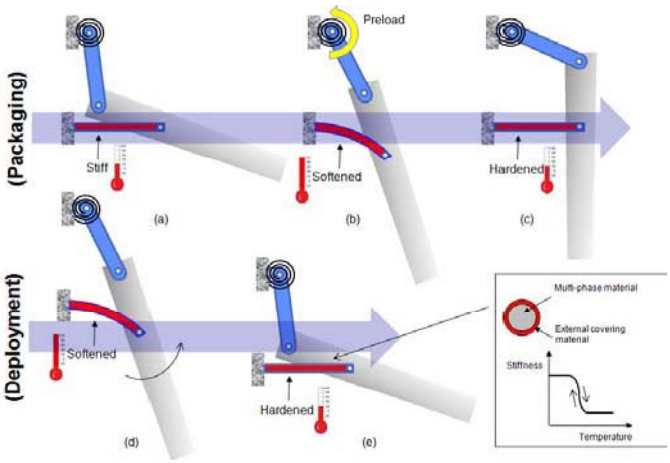

Figure 4: Bi-stable compliant mechanism[12]

The mechanism in Figure 4 is designed to have two stable positions, packaged and deployed. For transport, the wings are packaged or folded and stowed inside the UAV. Upon deployment and exposure to heat, the compliant link softens, allowing the spring loaded mechanism to rotate into the deployed position. The flexible link then cools and hardens locking the wing into position and increasing stability. Upon returning to base, the flexible link can then be re-activated and the vehicle packaged for storage or redeployment.

MODEL DEVELOPMENT

Vehicle Trajectory and Heating

To analyze the feasibility of such a system, vehicle launch characteristics are taken from the flight envelope of atypical high speed delivery vehicle, having a maximum altitude of 27,400m (90,000ft) and speed of Mach 3.35. These numbers are notional, and while realistic, do not represent any particular vehicle system. The deployed vehicle is assumed to have a diameter of 1m, lift to drag ratio of 2, drag coefficient of 1 (typical of a blunt body), a spherical nose, weigh approximately 300kg, have a length of 5m, and a uniform initial temperature.

The aerodynamic heating as a result of friction at supersonic speeds is calculated based on the characteristics of the stagnation properties of air behind a normal shock wave:[8,9]

$$\frac{\rho_2}{\rho_1} = \frac{u_1}{u_2} = \frac{M_1^2(1+\gamma)}{2+M_1^2(\gamma-1)} \qquad (1)$$

$$H_1 + \frac{u_1^2}{2} = H_2 + \frac{u_2^2}{2} \qquad (2)$$

where ρ is density, u is velocity, γ is the ratio of specific heats Cp/Cv, M is Mach number, and H is enthalpy. The subscripts *1* and *2* refer to free stream conditions and the

flow behind the shock wave respectively. Since the density of the air is known from Equation 1, the temperature and pressure of the air behind the shock wave are:

$$P_2 = P_1\left(1+\frac{2\gamma\left(M_1^2-1\right)}{\gamma+1}\right) \tag{3}$$

$$T_2 = T_1\frac{P_2}{P_1}\frac{\rho_1}{\rho_2} \tag{4}$$

The stagnation temperature of the flow is then:

$$T_{stag} = T_2\left(1+\frac{M_2^2(\gamma-1)}{2}\right) \tag{5}$$

Where:

$$M_2^2 = \frac{1+\frac{M_1^2(\gamma-1)}{2}}{\gamma M_1^2-\frac{(\gamma-1)}{2}} \tag{6}$$

Calculation of the heat flux into the vehicle is accomplished by the method described by Eckert by calculating an effective heat transfer coefficient and reference temperature[4]. The Reynolds number is calculated as:

$$\mathrm{Re} = \frac{\rho v D}{\mu} \tag{7}$$

where v is the free stream velocity of the vehicle, D is the diameter, and μ is the dynamic viscosity. The dynamic viscosity is calculated based on Sutherland's method by:[2]

$$\mu = \mu_0\frac{0.555T_0+C}{0.555T+C}\left(\frac{T}{T_0}\right)^{3/2} \tag{8}$$

where μ_0 and T_0 are reference viscosity and temperature (here taken as 0.01827 centipoise and 524.07R for air) respectively and C is Sutherland's constant, 120 for air. Equation 8 is accurate to within 10% up to a pressure of 500bar (5e7Pa) and over a temperature range of 0 to 1500F (255 to 1089K). To calculate the heat flux into the vehicle, Eckert[4] utilizes a fictitious reference temperature based on the stagnation point temperature of the flow:

$$T_{ref} = T_{stag}+\frac{v^2\sqrt{\mathrm{Pr}}}{2C_p} \tag{9}$$

where T_{stag} is the stagnation point temperature of the flow, Equation 5, *Pr* is Prandtl's number, taken as 0.71, and C_p is the specific heat capacity of air, $1000^{J}/_{kg*K}$. The effective coefficient of heat transfer is than calculated based on the Stanton number:

$$St = \frac{h}{\rho C_p v} = \frac{C_f}{2}(\mathrm{Pr})^{-2/3} \tag{10}$$

Rearranging Equation 10 yields:

$$h = 0.5C_f(\mathrm{Pr})^{-2/3}\rho C_p v \tag{11}$$

where h is the effective heat transfer coefficient, *St* is the Stanton number, and C_f is the coefficient of friction. The coefficient of friction is estimated by the Schuls-Grunow method as:[4]

$$C_f = \frac{0.370}{(\log_{10}\mathrm{Re})^{2.584}} \tag{12}$$

where *Re* is described by Equation 7. Finally, the heat flux into the vehicle at the stagnation point is calculated as:[4]

$$q_{stag} = h\left(T_{ref}-T_{surface}\right) \tag{13}$$

where q_{stag} is heat flux and $T_{surface}$ is the current temperature of the vehicle nose. The heat flux distribution over the entire nose of the vehicle is then calculated based on Lees method, where the ratio of the heat flux with respect to the heat flux at the stagnation point for a hemispherical body is:[3]

$$\frac{q}{q_0} = \frac{2\theta\sin(\theta)\left\{\left[1-\frac{1}{\gamma_\infty M_\infty^2}\right]\cos^2(\theta)+\frac{1}{\gamma_\infty M_\infty^2}\right\}}{\beta^{1/2}} \tag{14}$$

where θ is the angle between the analyzed point and the stagnation point ($0 \le \theta \le \pi/2$), ∞ designates a free stream quantity, and β is:

$$\beta = \left(1-\frac{1}{\gamma_\infty M_\infty^2}\right)\left(\theta^2-\frac{\theta\sin(4\theta)}{2}+\frac{1-\cos(4\theta)}{8}\right)+\frac{4}{\gamma_\infty M_\infty^2}\left(\theta^2-\theta\sin(2\theta)+\frac{1-\cos(2\theta)}{2}\right) \tag{15}$$

Figure 5, below, depicts Equation 14 evaluated over the nose of the vehicle at various speeds.

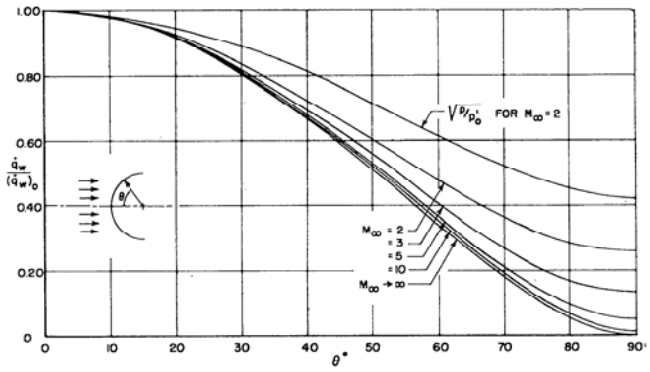

Figure 5: Heat flux ratio over nose at various speeds[3]

Thermal Heat Pipe Model

While the actual system, including the heat pipe, will be specifically designed to meet the exact criteria desired; the current feasibility effort employs a standard heat pipe design. The modeled heat pipe is a flat plate heat pipe with the evaporator section contoured to the nose of the vehicle as shown in Figure 6. Heated vapor exits the evaporator section and is directed through an adiabatic segment to the condenser section.

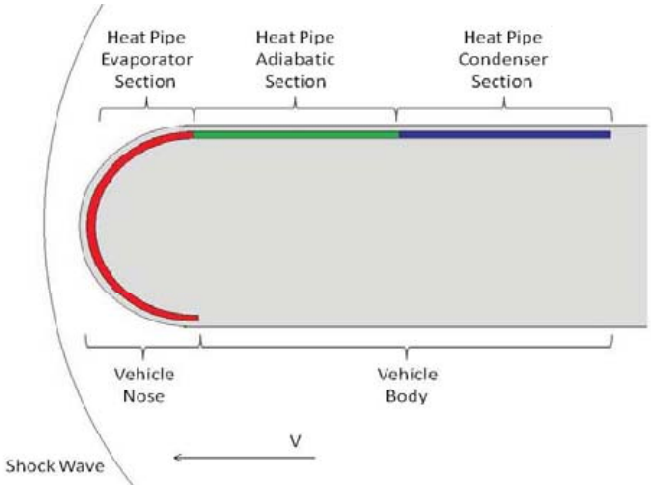

Figure 6: Heat pipe configuration

The heat pipe walls and wicks are constructed entirely of copper with water as the working fluid. The walls are 2mm thick (h_{wa}), wicks are 3mm thick (h_w), and the vapor channels are 5.5cm wide (W) and 10cm high (h_v), Figure 7. The evaporator section of the heat pipe is 1.1m square, while the adiabatic and condenser sections are arbitrary. Heat into the heat pipe in the evaporator section occurs only on the top surface of the heat pipe while the bottom (internally facing) surface is considered insulated.

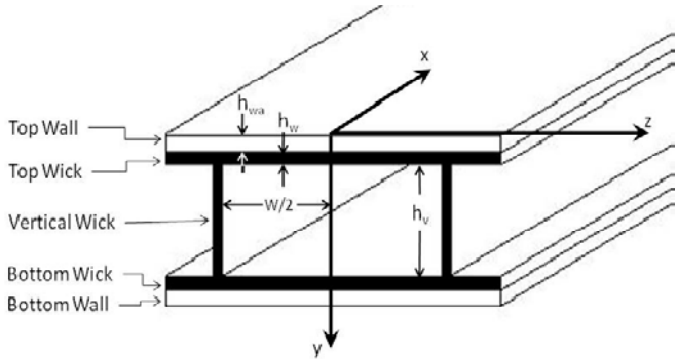

Figure 7: Heat pipe schematic

The heat equation is:

$$\rho C_p \frac{\partial T}{\partial t} = k\left(\frac{\partial^2 T}{\partial x^2} + \frac{\partial^2 T}{\partial y^2} + \frac{\partial^2 T}{\partial z^2}\right) \qquad (16)$$

where T is temperature, k is thermal conductivity, and x, y, and z are the three cardinal directions in an orthonormal basis. Equation 16 is often simplified by defining the thermal diffusivity as:

$$\alpha = \frac{k}{\rho C_p} \qquad (17)$$

To simplify the model, the wick of the heat pipe is modeled as a single material using effective material properties as described by Dunn and Reay[7]. Their equation describing the thermal conductance of the wick is:

$$k_w = k_{ws}\left[\frac{2 + \frac{k_{wl}}{k_{ws}} - 2\varepsilon_w\left(1 - \frac{k_{wl}}{k_{ws}}\right)}{2 + \frac{k_{wl}}{k_{ws}} + \varepsilon_w\left(1 - \frac{k_{wl}}{k_{ws}}\right)}\right] \qquad (18)$$

where ε is the porosity of the wick, 0.5, and the subscripts w, ws, and wl refer to the calculated effective wick property and properties of the solid and liquid materials comprising the wick respectively. Other quantities such as the wick density and heat capacity are calculated analogously. The boundary conditions of the heat pipe are:

$$-k_{wa}\left.\frac{\partial T_e}{\partial y}\right|_{y=0} = q_{in} \qquad (19)$$

$$-k_{wa}\left.\frac{\partial T_e}{\partial y}\right|_{y=h_{wa}} = -k_w\left.\frac{\partial T_e}{\partial y}\right|_{y=h_{wa}} = q_{wwe} \qquad (20)$$

$$-k_w = \left.\frac{\partial T_e}{\partial y}\right|_{y=h_w+h_{wa}} q_v \qquad (22)$$

where the subscripts *w*, *wa*, *e*, *v*, and *wwe* refer to the heat pipe wick, wall, evaporator, wick/vapor interface, and wall/wick interface in the evaporator respectively. The dimension *y* is the thickness direction having $y = 0$ the heat pipe surface, $y = h_{wa}$ the wall/wick interface, and $y = h_{wa}+h_w$ the wick/vapor interface. q_{in} in Equation 19 is the heat into the heat pipe while q_v in Equation 22 represents the heat flux associated with the production of vapor and thus the thermal energy delivered to the internal mechanics responsible for wing deployment.

MODEL RESULTS

Vehicle Trajectory and Heat Load

The calculated trajectory for the vehicle having a lift to drag ratio of 2, a diameter of 1m, weighing approximately 300kg, and a length of 5m is pictured below in Figure 8.

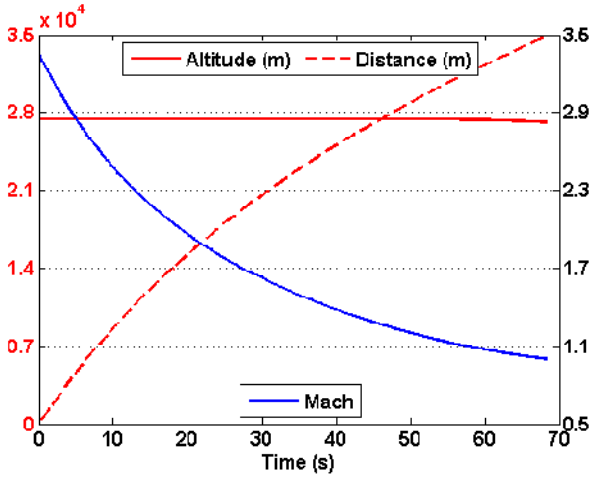

Figure 8: Example trajectory of deployed vehicle

The initial speed of the vehicle when deployed is Mach 3.35 at an altitude of 27.4km. Due to the thin atmosphere at this altitude and an appreciable lift to drag ratio, the vehicle descends little before decreasing below Mach 1.0 despite travelling approximately 35km in approximately 68 seconds. To calculate the heat flux into the vehicle, the coefficient of friction and Reynolds numbers over the trajectory must first be calculated and are shown in Figure 9.

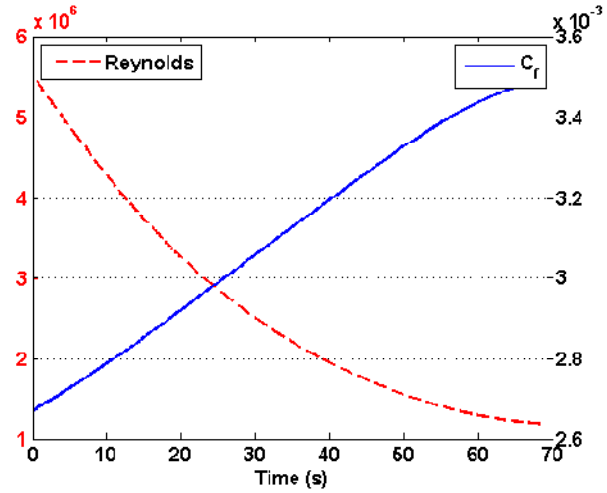

Figure 9: Coefficient of friction and Reynolds numbers

Once these are known, Eckert's method of calculating the heat flux into the vehicle via an effective heat transfer coefficient and reference temperature results in the coefficient of heat transfer with respect to time shown below in Figure 10 with the heat flux calculated using Equation 13.

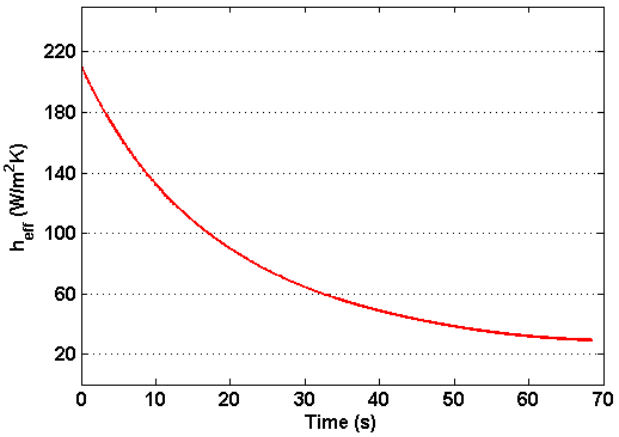

Figure 10: Effective heat transfer coefficient of the vehicle

Once the heat input to the vehicle is known, the internal thermal distribution is calculated via the method described by Vafai et. al.[5,6,7] The resulting model then describes time dependant temperature characteristics of the heat pipe from the nose of the vehicle to the desired internal location.

Thermal Model Results

With a complete model, the temperature on the surface of the nose of the vehicle as well as the internal temperatures can be calculated. The temperature distribution over the nose of the aircraft, which is the same as the distribution over the flat plate heat pipe, soon after deployment is shown below in Figure 11.

Figure 12, then is a graph showing the evolution of temperature as a function of time.

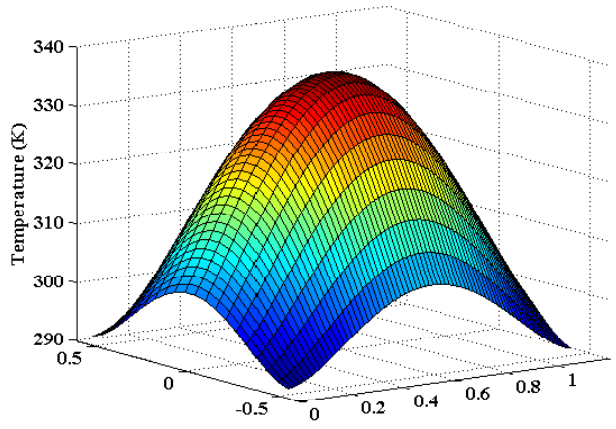

Figure 11: Temperature distribution over nose of vehicle

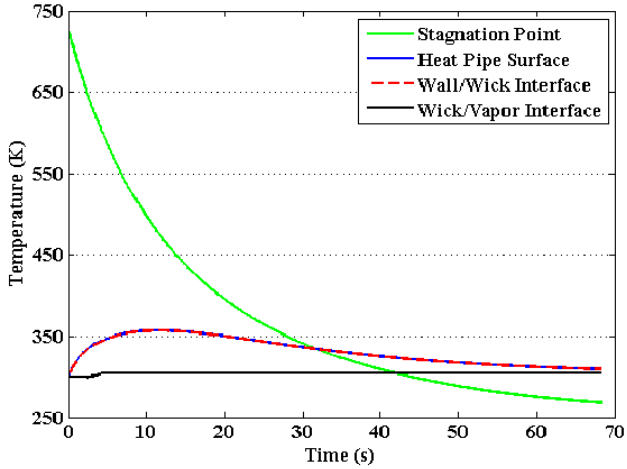

Figure 12: Evolution of temperature in the evaporator section

With an initial temperature of 300K, the maximum temperatures of the external skin of the vehicle as well as the wall/wick interface are approximately 360K 10 seconds after deployment. The difference between the surface of the heat pipe and the wall/wick interface is within one degree for the entire simulation. The boiling temperature of the working fluid, adjustable based on the fluid used and the internal pressure of the heat pipe, is arbitrarily prescribed to be 305K. A low boiling temperature ensures maximum vapor creation and thus heat transfer, although limits the transition temperature of the flexible link described above. The temperature of the wick/vapor interface begins to increase at approximately 2.5 seconds, increases to 305K in 2 seconds, and is held constant at the boiling temperature for the remainder of the simulation. In future work, this boiling temperature will vary with varying internal pressure of the heat pipe.

Figure 13, below, shows the temperature distribution through the thickness of the evaporator section of the heat pipe at several times.

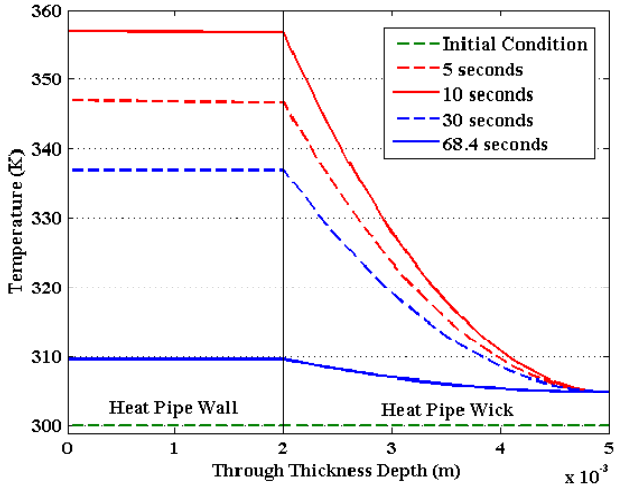

Figure 13: Temperature distribution through the heat pipe

The vertical line in Figure 13 designates the wall/wick interface. 0 to 2mm is the temperature distribution in the evaporator wall while 2mm to 5mm is the temperature distribution in the wick of the heat pipe. Figures 12 and 13 clearly show that as the vehicle slows, the temperature of the surface decreases. This is due to the exterior temperature created behind the shock wave decreasing over time with reducing speed. Figure 14 shows the heat flux into the vehicle, at the wall/wick interface, and the wick/vapor interface for the entire simulated flight.

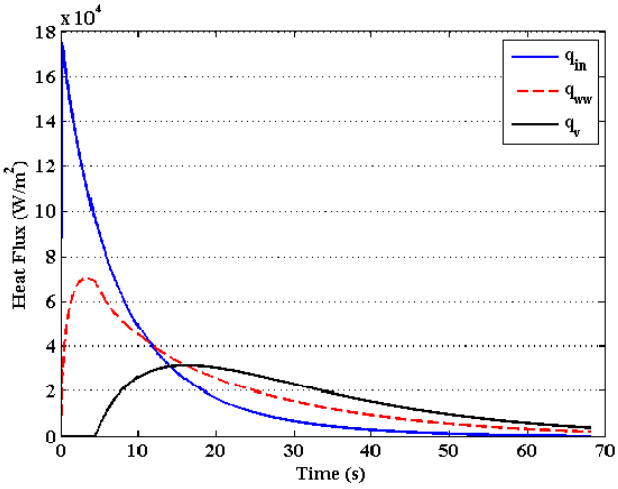

Figure 14: Heat flux through the heat pipe

Over the entire trajectory, of the 445kJ entering the heat pipe, approximately 375kJ is transferred and utilized to create vapor during the 68 second flight, representing a thermal efficiency of 84%. While energy losses incurred while the vapor travels from the evaporator to the

condenser and the losses associated with transferring the thermal energy to the physical link are not accounted for, the energy efficiency of the system exceeds that of typical thermoelectric and pyroelectric devices.

DISCUSSION/CONCLUSION

While the presented model and results represent a respectable solution to assess the feasibility of a direct thermal use deployment scheme for the high speed deployment of low speed ISR assets, there are many factors not accounted for in the model that may be improved. The material properties of the heat pipe are not modeled as temperature dependant, which could affect the overall performance of the system. Thermal shock of the system is also not considered. The design of the heat pipe, namely the materials used and geometry have not been optimized for the analyzed trajectory which may enable better system efficiency. The example case is based on a notional deployment speed and altitude, and a given set of deployed vehicle lift/drag ratio and mass. The ability to control the deployed vehicle prior to wing deployment would allow control of the external heat environment in terms of increasing the maximum temperatures attained as well as the length of time the vehicle collects thermal energy, making the system more advantageous. As mentioned previously, the temperature and thus the heat transfer could also be increased by changing the shape of the nose of the vehicle to be less spherical.

The presented analyzed trajectory results in the delivery of 375kJ to the desired internal wing deployment mechanism. As a reference, Lee et al.[13] report the heat of crystallization of a particular SMP to be up to 324 J/g. 375kJ would then be able to transition up to 1.1kg of material, or approximately 1050cm3. 375kJ delivered over 68 seconds also is equivalent to operating a 7.35hp electric motor for the same duration or a standard 20hp motor for 25 seconds.

Other factors in the feasibility of the system not discussed here include the weight difference between a direct thermal use system, the presented design weighing approximately 40kg (88bs), and alternative actuation schemes such as a more typical electric motor driven system which would in turn effect the efficiency of the aircraft once deployed. Any adverse effects, such as weight or physical space taken by the system and thus not available for other uses would have to be weighed against system readiness and complexity.

As the speed and altitude of deployment increase, increasing the thermal energy available for harvesting, the advantages of the presented system become greater since the size and weight of the system remain constant but the amount of delivered energy increases proportionately. Alternatively, the size and weight of a traditional system requiring on-board energy storage scales with the amount of stored energy desired. The presented method and model serve as a means to quantitatively evaluate the feasibility and design of a direct use thermal transport system while simultaneously providing a means of design and optimization of the heat pipe geometry.

Lastly, the presented model does not account for the transient response of the vapor inside the heat pipe. While this capability is currently being worked on, from previous publications a reasonable assumption is to add approximately a 6 second delay between the thermal energy exiting the evaporator section and reaching the flexible link mechanism. This is significant given a flight envelope of only 68 seconds.

ACKNOWLEDGMENTS

Financial support for the project by Dr. Les Lee in AFOSR is graciously acknowledged.

REFERENCES

[1] Dewey, T.J., Cheatem, L.T., and Howe, H., 2004, "Vegetable Oil-Based Lubricants for Stable Operation up to 1000°C," *Bull. Eng. Trib.*, **24**(2), pp. 45-54.

[2] Crane Co., 1988, "Flow of Fluids Through Valves, Fittings, and Pipe", Technical Paper No. 410

[3] Lees, Lester, 1956, "Laminar Heat Transfer Over Blunt-Nosed Bodies at Hypersonic Flight Speeds", *AIAAJournal Special Supplement: Centennial of Powered Flight*, vol. 26, no. 4, pp. 259-269

[4] Eckert, Ernst R. G, 1961, "Survey on Heat Transfer at High Speeds", *Aeronautical Research Laboratory, Office of Aerospace Research, USAF, Wright-Patterson AFB, Ohio*

[5] Zhu, N., Vafai, K., 1997, "Analytical modeling of the startup characteristics of asymmetrical flat-plate and disk-shaped heat pipes", *International Journal of Heat and Mass Transfer*, vol. 41, no. 17, pp 2619-2637

[6] Wang, Y., Vafai, K, 2000, "Transient characterization of flat plate heat pipes during startup and shutdown operations", *International Journal of Heat and Mass Transfer*, vol. 43, pp 2641-2655

[7] Zhu, N., Vafai, K., 1997, "Vapor and liquid flow in a asymmetrical flat plate heat pipe: a three dimensional analytical and numerical investigation", *International Journal of Heat and Mass Transfer*, vol. 41, no. 1, pp 159-174

[8] Anderson, J., 1989, "Hypersonic and High Temperature Gas Dynamics", *McGraw-Hill*, New York

[9] White, F., 1991, "Viscous Fluid Flow 2nd edition", *McGraw-Hill*, New York

[10] Dunn, P. D., Reay, D. A., 1982, "Heat Pipes, 3rd edition", *Pergamon Press*, New York

[11] 6 May 2010, http://www.cheresources.com/htpipes.shtml

[12] Joo, J. J., Robertson, D., Smyers, B. M., Reich, G. W., 2010, "Thermally-Activated Reconfigurable Wing Design Using a Non-Monolithic Compliant Mechanism", 51st AIAA/ASME/ASCE/AHSs/ASC Structures, Structural Dynamics & Materials Conference, April 12-15, AIAA 2010-2665, Orlando, Florida

[13] Lee, B. S., Chun, B. C., Chung, Y. C., Sul, K. I., and Cho, J. W., "Structure and Thermomechanical Properties of Polyurethane Block Copolymers With Shape Memory Effect", *Macromolecules*, vol. 34, pp 6431-6437